Dimeric Procaspase-3 Unfolds via a Four-State Equilibrium Process†

Kakoli Bose and A. Clay Clark*

Department of Molecular and Structural Biochemistry, North Carolina State University, Raleigh, North Carolina 27695

Received May 21, 2001; Revised Manuscript Received August 13, 2001

ABSTRACT: We have examined the folding and assembly of a catalytically inactive mutant of procaspase-3, a homodimeric protein that belongs to the caspase family of proteases. The caspase family, and especially caspase-3, is integral to apoptosis. The equilibrium unfolding data demonstrate a plateau between 3 and 5 M urea, consistent with an apparent three-state unfolding process. However, the midpoint of the second transition as well as the amplitude of the plateau are dependent on the protein concentration. Overall, the data are well described by a four-state equilibrium model in which the native dimer undergoes an isomeration to a dimeric intermediate, and the dimeric intermediate dissociates to a monomeric intermediate, which then unfolds. By fitting the four-state model to the experimental data, we have determined the free energy change for the first step of unfolding to be 8.3 ± 1.3 kcal/mol. The free energy change for the dissociation of the dimeric folding intermediate to two monomeric intermediates is 10.5 ± 1 kcal/mol. The third step in the unfolding mechanism represents the complete unfolding of the monomeric intermediate, with a free energy change of 7.0 ± 0.5 kcal/mol. These results show two important points. First, dimerization of procaspase-3 occurs as a result of the association of two monomeric folding intermediates, demonstrating that procaspase-3 dimerization is a folding event. Second, the stability of the dimer contributes significantly to the conformational free energy of the protein (18.8 of 25.8 kcal/mol).

The clear understanding of a biological concept requires insights from physical chemistry. While it has been observed that the biological activity of a protein is dependent on its ability to fold into the correct three-dimensional structure, predicting the correct fold of a protein based solely on its primary sequence, the so-called "protein folding problem", has been elusive. The problem will become critical in the post-genomic age for gaining precise information on intricate biological functions of proteins.

As first shown by Anfinsen (*1*) and later pointed out by Baker (*2*), the simplest case of biological self-organization is the spontaneous self-assembly of protein molecules into a unique three-dimensional structure that carries out biological function. While great interest in this area over the past few decades has resulted in a plethora of experimentation (*3*), most of the experimental systems have been confined to small single-domain proteins (*4*). For most of those proteins, partially ordered non-native conformations, that is, folding intermediates, are not typically observed. The folding could be well modeled as a two-state transition between a denatured state and the ordered native state. While these models provide a framework for solutions to the folding problem, they cannot account for the complexities of folding of multidomain or multisubunit proteins. One challenge that underlies protein folding studies in the onset of proteomics is to correlate the functional features found in protein families with the evolutionary conservation of sequence identity (*5*) as well as conserved structural topology (*2*). While models of contact order (*2*) and conservatism (*5*) have been developed using small proteins with well-characterized two-state folding transitions, eventually these or other models must be extended to larger multidomain or multisubunit proteins. A complete understanding of folding and assembly will fully reflect the balance between local and global interactions, including global interactions between subunits.

Because of these and other considerations, we have examined the folding and assembly of procaspase-3, which belongs to the caspase family of proteases. Caspase [cysteinyl aspartate-specific protease (*6*)] family members are key mediators of initiation and execution of apoptosis as well as the inflammatory response. Currently, 14 members of the caspase family have been identified (*7*), and crystal structures of several caspases demonstrate the structural homology within the family (*8*−*14*). The mature, enzymatically active caspases are tetramers with a M_r of approximately 60 000 and consist of two copies each of two nonidentical subunits, described as dimers of heterodimers. Caspases exist in normal cells as inactive zymogens and must be activated by proteolytic processing [for a review, see Salvesen (*15*)]. While the three-dimensional structures have not been determined, the monomeric procaspase polypeptides are organized with an amino-terminal pro-domain, which varies in size and function, followed by the large subunit and the small subunit. In some cases, such as procaspase-1, an intersubunit linker is found between the subunits within the procaspase (*16*). The caspase family can be divided into two important subclasses based on the size of the pro-domain; the long pro-domain caspases are generally activators in the apoptosis cascade, whereas the short pro-domain caspases are generally

† This work was supported by a grant from the American Diabetes Association.

* To whom correspondence should be addressed at the Department of Molecular and Structural Biochemistry, 128 Polk Hall, North Carolina State University, Raleigh, NC 27695-7622. Phone: (919) 515-5805. Fax: (919) 515-2047. E-mail: clay_clark@ncsu.edu.

10.1021/bi0110387 CCC: $20.00
Published on Web 10/26/2001

executioners in cell death. While the pro-domain for long pro-domain caspases has been shown to facilitate protein−protein interactions that lead to maturation (*17, 18*), the role of the pro-domain, if any, in dimerization and maturation of the short pro-domain caspases is less clear.

Consistent with models for maturation of the long pro-domain caspases (*19, 20*), our finding that procaspase-3 is a dimer in solution (*44*) suggests that dimerization is an early event in maturation of the short pro-domain caspases. That is, the procaspase dimer, rather than the monomer, is cleaved. This is important because the four subunits in the caspase heterotetramer reside in one procaspase dimer. However, those experiments did not address procaspase-3 dimerization in the context of folding, that is, whether the dimer forms from two native monomers or whether dimerization occurs during folding. In the results presented here, we have analyzed the equilibrium folding of the procaspase-3 dimer in urea-containing phosphate buffer using spectroscopic probes that are sensitive to changes in the secondary and tertiary structures. Overall, the data are well described by a four-state equilibrium model in which the native dimer undergoes an isomeration to a dimeric intermediate, and the dimeric intermediate dissociates to a monomeric intermediate, which then unfolds ($N_2 \rightleftharpoons I_2 \rightleftharpoons 2I \rightleftharpoons 2U$). The data demonstrate that dimerization of procaspase-3 occurs during folding by the association of partially folded monomeric species.

MATERIALS AND METHODS

Protein Purification. Procaspase-3 (C163S) was isolated from *E. coli* BL21(DE3) as described previously (*44*). The concentration was determined using $\epsilon_{280} = 26\,500\ M^{-1}\ cm^{-1}$ (*44*). The protein concentrations reported here are those of the monomer.

Reagents. Ultrapure urea was purchased from Nacalai Tesque Inc. (Kyoto, Japan). Dithiothreitol (DTT) and potassium phosphate (KH_2PO_4 and K_2HPO_4) were obtained from Sigma Chemicals (St. Louis, MO). All other chemicals were reagent-grade.

Stock Solutions. Urea stock solutions (10 M) were prepared as described previously (*21*) in a buffer of 50 mM KH_2PO_4/K_2HPO_4, pH 7.2 (±0.01), 1 mM DTT. This buffer solution without urea is referred to as "phosphate buffer" in the text. All solutions were prepared fresh for each experiment and were filtered (0.22 μm pore size) prior to use. The urea concentration of each stock solution was calculated by weight and by refractive index (*21*), and solutions were used only if the two values were within ±1%.

Equilibrium Unfolding Studies. All equilibrium unfolding experiments were performed as described previously (*21, 22*). Briefly, stock protein solutions were prepared in phosphate buffer to be 10 times the final concentration used in the experiment. Phosphate buffer, urea from the 10 M stock solution, and stock protein solutions were mixed in 2 mL siliconized microcentrifuge tubes (Sigma Chemicals) to give final urea concentrations between 0 and 8 M and the final protein concentrations as indicated in the figure legends. For renaturation experiments, the protein was incubated in 6 M urea-containing phosphate buffer. After incubation for 1 h at 25 °C, the protein was added to phosphate buffer and urea such that the final urea and protein concentrations were as indicated in the figure legends. All samples were mixed by vortexing. To determine that the samples had reached equilibrium, we monitored the fluorescence emission over time for a sample incubated in 4 M urea-containing phosphate buffer. The results from this experiment (data not shown) demonstrate that the sample equilibrated within 45 min at 25 °C as there was no further change in signal after this time. When the protein was refolded by dilution from 8 to 0.8 M urea, we observed several kinetic phases, although folding was complete within several hours. For the equilibrium unfolding experiments, the samples were incubated for approximately 24 h at 25 °C prior to data collection. This incubation time was sufficient to allow all samples to equilibrate.

Fluorescence emission at each denaturant concentration was measured using a PTI C-61 spectrofluorometer (Photon Technology International). Time-based measurements were acquired at excitation wavelengths of 280 and 295 nm with fluorescence emission at 320 nm. All measurements were corrected for background signal. Circular dichroism at 228 nm was measured with a Jasco J600A spectropolarimeter using a cuvette of 1 cm path length. The data were averaged for 30 s. Both instruments were equipped with thermostated cell holders, and the temperature was held constant at 25 °C using a circulating water bath.

Data Analysis. The fluorescence and circular dichroism studies were modeled using the four-state equilibrium model shown in eq 1:

$$N_2 \overset{K_1}{\rightleftharpoons} I_2 \overset{K_2}{\rightleftharpoons} 2I \overset{K_3}{\rightleftharpoons} 2U \tag{1}$$

In this model, the protein is assumed to be in either the native homodimeric state (N_2), a non-native dimeric state (I_2), a non-native monomeric state (I), or an unfolded monomeric state (U), and K_1, K_2, and K_3 are the equilibrium constants for the three steps, respectively. If we consider the total molar concentration of the polypeptide chains as P_T, as shown in eq 2:

$$P_T = 2[N_2] + 2[I_2] + [I] + [U] \tag{2}$$

then the mole fraction of each species can be defined as shown in eqs 3−6:

$$f_{N_2} = \frac{2N_2}{P_T} \tag{3}$$

$$f_{I_2} = \frac{2I_2}{P_T} \tag{4}$$

$$f_I = \frac{I}{P_T} \tag{5}$$

$$f_U = \frac{U}{P_T} \tag{6}$$

The sum of all fractions is equal to unity as shown in eq 7:

$$f_{N_2} + f_{I_2} + f_I + f_U = 1 \tag{7}$$

The equilibrium constants K_1, K_2, and K_3 are related to the

mole fraction of each species and to P_T, as shown in eqs 8−10:

$$K_1 = \frac{f_{I_2}}{f_{N_2}} \quad (8)$$

$$K_2 = \frac{2f_I^2 P_T}{f_{I_2}} \quad (9)$$

$$K_3 = \frac{f_U}{f_I} \quad (10)$$

Equating eqs 8−10, substituting in terms of f_U, and rearranging yield eq 11:

$$\frac{2f_U^2 P_T}{K_2 K_3^2 K_1} + \frac{2f_U^2 P_T}{K_2 K_3^2} + \frac{f_U}{K_3} + f_U - 1 = 0 \quad (11)$$

By solving the quadratic eq 11, the fraction of each species is obtained, as shown in eqs 12−15:

$$f_U = \{-K_1K_2K_3(1+K_3) + \sqrt{K_1^2K_2^2K_3^2(1+K_3)^2 + 8P_T(1+K_1)(K_1K_2K_3^2)}/4P_T(1+K_1)\} \quad (12)$$

$$f_I = \frac{f_U}{K_3} \quad (13)$$

$$f_{I_2} = \frac{2f_I^2 P_T}{K_2} \quad (14)$$

$$f_{N_2} = \frac{f_{I_2}}{K_1} \quad (15)$$

From eqs 12−15 and the relationship

$$\Delta G = -RT \ln(K_{eq}) \quad (16)$$

where R is the gas constant and T is the temperature in degrees kelvin, one may calculate the equilibrium constant and the values of ΔG at each urea concentration. We assume the free energy change for each step in the reaction to be linearly dependent on denaturant concentration as described earlier (*23*) (eqs 17−19):

$$\Delta G_1 = \Delta G_1^{H_2O} - m_1[\text{denaturant}] \quad (17)$$

$$\Delta G_2 = \Delta G_2^{H_2O} - m_2[\text{denaturant}] \quad (18)$$

$$\Delta G_3 = \Delta G_3^{H_2O} - m_3[\text{denaturant}] \quad (19)$$

where $\Delta G_1^{H_2O}$, $\Delta G_2^{H_2O}$, and $\Delta G_3^{H_2O}$ are the free energy changes in the absence of denaturant corresponding to K_1, K_2, and K_3, respectively, and m_1, m_2, and m_3 are the cooperativity indices associated with each step. The amplitude of the spectroscopic signal determined at each urea concentration is assumed to be a linear combination of the fractional contribution from each species (eq 20):

$$Y = Y_{N_2}f_{N_2} + Y_{I_2}f_{I_2} + Y_I f_I + Y_U f_U \quad (20)$$

where Y_{N_2}, Y_{I_2}, Y_I, and Y_U are the amplitudes of the signals for the respective species.

To determine the unknown parameters $\Delta G_1^{H_2O}$, $\Delta G_2^{H_2O}$, $\Delta G_3^{H_2O}$, m_1, m_2, and m_3, the 10 data sets shown in Figures 2 and 3 were fit simultaneously using Igor Pro. For each spectroscopic signal, the values for Y_{I_2} and Y_I did not vary with changes in P_T. The following values were determined from the fits. For fluorescence emission (280 nm excitation), $Y_{I_2} = 0.78$ and $Y_I = -0.16$. For circular dichroism at 228 nm, $Y_{I_2} = 0.85$ and $Y_I = 0.3$. For fluorescence emission (295 nm excitation), $Y_{I_2} = 1.13$ and $Y_I = 0.08$. The amplitudes associated with the native form of the protein were assumed to be linearly dependent on urea concentration, as shown in eq 21:

$$Y_{N_2} = Y_{N_2'} + m_4[\text{urea}] \quad (21)$$

where $Y_{N_2'}$ is the amplitude of the signal in the absence of urea for the native species. This correction to the pre-transition baselines (eq 21) had little effect on the free energy or *m*-values determined from the fits. For example, when m_4 was set to 0, $\Delta G_1^{H_2O}$ varied from 8.3 to 7.5 kcal/mol, and m_1 varied from 2.8 to 2.65 kcal mol^{-1} M^{-1}. The remaining parameters were unchanged. These variations in $\Delta G_1^{H_2O}$ and m_1 are within the experimental error. The fits shown in Figures 2 and 3 as well as the values reported in the text reflect the pre-transition baseline corrections. Due to the lack of a sufficient number of data points in the post-transition regions, no corrections were made to the post-transition baselines, and the values of Y_U were set to 0, in agreement with the normalized experimental data shown in the Figures 2 and 3. The values of P_T were not allowed to vary during the fitting process.

RESULTS

The monomeric procaspase-3 consists of 277 amino acids (M_r = 31 577). Under some conditions, such as the high protein concentrations found in heterologous expression systems, caspase-3 activation is autocatalytic (*24*−*26*). To prevent autoproteolysis, we substituted the active site cysteine with a serine residue (C163S) for our equilibrium unfolding studies. The C163S mutation prevents autolysis of the procaspase but is not structurally perturbing (*20*, *27*, *28*).

Denaturation of Procaspase-3(C163S). While there are no aromatic residues in the pro-domain, procaspase-3 has two tryptophan residues (W206 and W214), and both reside in the carboxy-terminal region of the polypeptide, that is, the region that becomes the small subunit of the mature caspase. In addition, there are 10 tyrosine residues well distributed in the primary sequence. Based on these features, it is convenient to examine folding and unfolding of the tertiary structure by monitoring changes in fluorescence emission.

As shown in Figure 1, native procaspase-3(C163S) has a fluorescence emission maximum at 335 nm when excited at 280 nm (panel A) and 340 nm when excited at 295 nm (panel B), indicating that the tryptophans are more solvent-exposed than the remaining aromatic residues. In the mature caspase-3 heterotetramer, the tryptophans are in or near the active site. Based on results from limited trypsin proteolysis of pro-

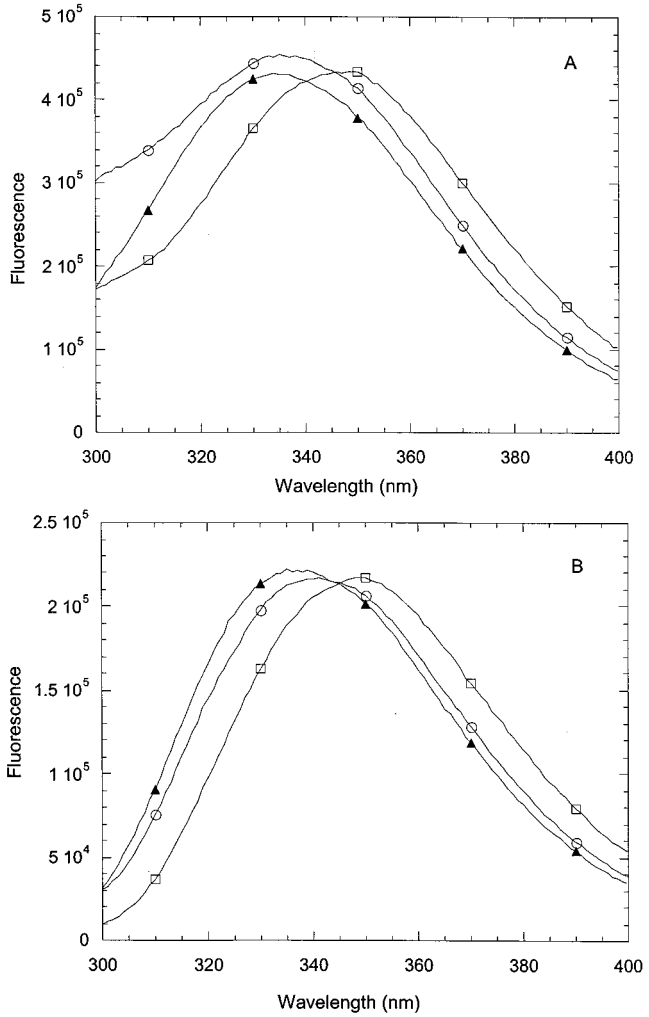

FIGURE 1: Fluorescence emission spectra of procaspase-3(C163S). Panel A: Excitation at 280 nm. Panel B: Excitation at 295 nm. Procaspase-3(C163S) (2 μM) was incubated for 24 h, 25 °C, in urea-containing phosphate buffer with the following urea concentrations: 0 M (○), 4 M (▲), 8 M (□).

caspase-3 (data not shown), the conformation of the procaspase-3 dimer appears to be similar to that of the heterotetramer. This suggests that in procaspase-3, the two tryptophan residues are in or near the active site and explains the red-shift in fluorescence emission (Figure 1, panel B) compared to the protein excited at 280 nm (Figure 1, panel A). In phosphate buffer containing 8 M urea, the fluorescence emission maximum is red-shifted to approximately 348 nm following excitation at either 280 nm (Figure 1, panel A) or 295 nm (Figure 1, panel B), indicating that the protein was largely unfolded under these solution conditions. In addition, the fluorescence intensity does not change dramatically. The far-UV circular dichroism spectrum of procaspase-3(C163S) demonstrates a large β-sheet content, whereas the near-UV CD spectrum demonstrates a well-defined packing of the aromatic side chains (*44*). In 8 M urea-containing phosphate buffer, both near-UV and far-UV CD spectra show a large signal change due to loss of secondary and tertiary structure (data not shown).

At intermediate concentrations of urea (~3−5 M), the fluorescence emission spectra were blue-shifted compared to those for the native protein. Representative data are shown in Figure 1 (panels A and B) for protein in 4 M urea-containing phosphate buffer. Under these conditions, the emission maxima were either 337 nm (panel B) or 333 nm (panel A). These results suggested the presence of an equilibrium folding intermediate that is populated under these conditions (3−5 M urea).

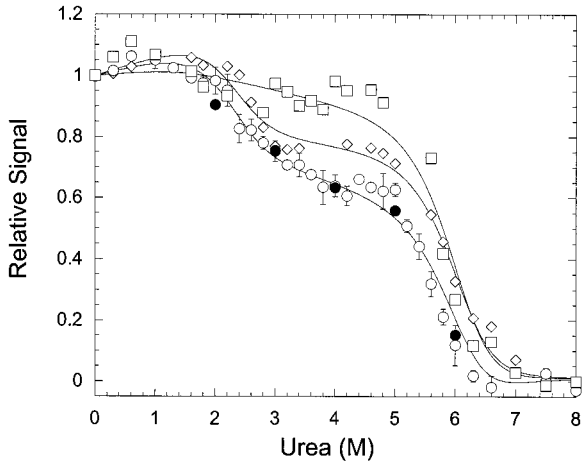

FIGURE 2: Equilibrium unfolding of procaspase-3(C163S). Unfolding was measured by CD at 228 nm (◇) and by fluorescence emission at 320 nm with excitation at either 280 nm (○) or 295 nm (□). For all experiments, the protein concentration was 1 μM. Closed symbols (●) represent refolded protein to show reversibility. Error bars show the standard error from four unfolding curves. For clarity, error bars and refolding data are not shown for all three data sets. The data were fit simultaneously (solid lines) as described under Materials and Methods using Igor Pro.

Equilibrium Unfolding of Procaspase-3(C163S). We examined the equilibrium unfolding of procaspase-3(C163S) in phosphate buffer as a function of urea concentration (0−8 M), and the results are shown in Figure 2. In these experiments, we monitored changes in secondary structure by circular dichroism at 228 nm and changes in tertiary structure by fluorescence emission at 320 nm, following excitation at 280 or 295 nm. The data show little to no change in signal between 0 and ~1.5 M urea, and this is followed by a cooperative decrease in signal from ~1.5 to ~3 M urea. A second cooperative transition occurs between ~5 and 7 M urea. While all three spectroscopic signals showed similar trends in the unfolding data, the relative signal in the plateau region (3−5 M urea) was significantly higher when the samples were excited at 295 nm (Figure 2, squares) compared to either the CD (diamonds) or the fluorescence emission with excitation at 280 nm (circles). The error bars in Figure 2 represent the standard error obtained from four different experiments at 1 μM concentration of procaspase-3(C163S) performed on separate days, demonstrating the reproducibility of the experiments.

To examine reversibility, the protein was initially unfolded in phosphate buffer containing either 6 or 8 M urea, and the samples were diluted into phosphate buffer so that the final protein concentration was 1 μM, and the final urea concentrations are shown in Figure 2 (solid circles). The data demonstrate the folding transitions are completely reversible.

Overall, the data shown in Figure 2 demonstrate at a minimum a three-state unfolding process in which a well-populated folding intermediate is in equilibrium with the native and unfolded protein.

Protein Concentration Dependence of Unfolding. Because procaspase-3 is a homodimer (*44*), we examined the effect

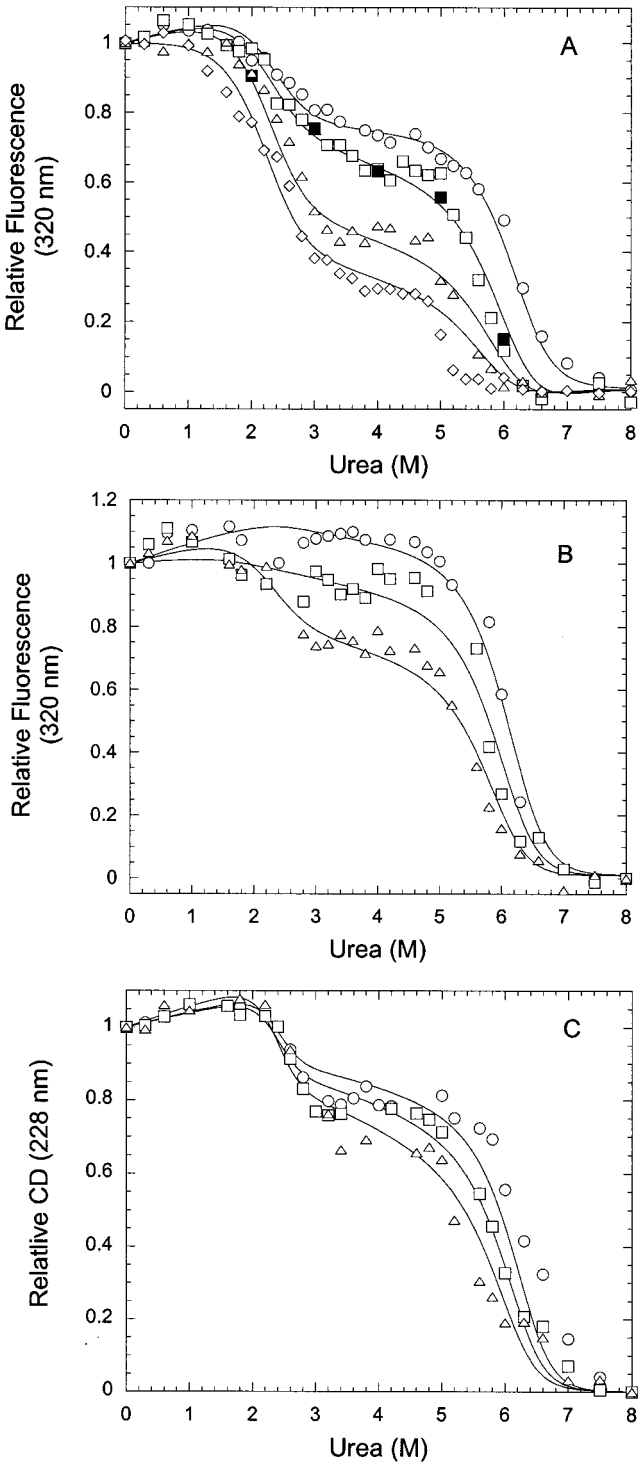

FIGURE 3: Concentration dependence of equilibrium unfolding of procaspase-3(C163S). For panels A and B, unfolding was monitored by fluorescence emission at 320 nm with excitation at 280 nm (panel A), or 295 nm (panel B), at protein concentrations of 0.25 μM (◇), 0.5 μM (△), 1 μM (□), and 2 μM (○). Closed symbols (■) represent refolding of procaspase-3 (C163S) at 1 μM concentration. For panel C, unfolding was monitored by CD at 228 nm at protein concentrations of 0.5 μM (△), 1 μM (□), and 2 μM (○). The data were fit simultaneously (solid lines) as described under Materials and Methods using Igor Pro.

of protein concentration on the equilibrium unfolding process. As shown in Figure 3, panels A−C, there was a shift in the midpoint of the second transition as the concentration of procaspase-3(C163S) was increased. Circular dichroism measurements at 228 nm (Figure 3, panel C) showed that the first transition was independent of the protein concentration.

The unusual feature of these data is that the relative amplitude of the plateau was dependent on the protein concentration. For example, as shown in Figure 3, panel A, the relative amplitude of the plateau decreased with a decrease in protein concentration, while the midpoint of the first transition was constant at ~2.4 M urea.

The results shown in Figure 3 suggest the four-state equilibrium model described in eq 1 (see Materials and Methods). In this model, the dimeric native conformation, N_2, isomerizes to a dimeric intermediate, I_2, and the dimeric intermediate dissociates to a monomeric intermediate, I, which unfolds to U. The dissociation of I_2 to 2I leads to a change in the amplitude of the plateau.

Based on this model, we have determined the conformational free energy, ΔG^{H_2O}, and the cooperativity indices, or *m*-values, for each step in unfolding (see Materials and Methods). The solid lines in Figures 2 and 3 are the results of fits of the model in eq 1 to the data. These results demonstrate that the data are well described by the four-state equilibrium model.

The free energy change, $\Delta G_1^{H_2O}$, and the cooperativity index, m_1, for the first step of unfolding, the isomerization of $N_2 \rightleftarrows I_2$, are 8.3 ± 1.3 kcal/mol and 2.8 ± 0.5 kcal mol^{-1} M^{-1}, respectively. The free energy change, $\Delta G_2^{H_2O}$, and cooperativity index, m_2, for the dissociation of the dimeric intermediate to two monomeric intermediates ($I_2 \rightleftarrows 2I$) are 10.5 ± 1.0 kcal/mol and 0.5 ± 0.1 kcal mol^{-1} M^{-1}, respectively. The third step in the unfolding mechanism represents the complete unfolding of the monomeric intermediate ($2I \rightleftarrows 2U$), with a free energy change, $\Delta G_3^{H_2O}$, and cooperativity index, m_3, of 7.0 ± 0.5 kcal/mol and 1.2 ± 0.1 kcal mol^{-1} M^{-1}, respectively. Overall, the data demonstrate that procaspase-3(C163S) is very stable, with total conformational free energy of 25.8 kcal/mol.

The plateau observed between 3 and 5 M urea (Figure 3) is due to the dissociation of the dimeric intermediate, I_2, to the stable monomeric intermediate, I. As shown in Figure 3, this plateau is relatively flat. The fits of the data show that this is due to two factors. First, the cooperativity index, m_2, for this process is relatively small, 0.5 kcal mol^{-1} M^{-1}. Using eqs 16 and 18 and the values determined for $\Delta G_2^{H_2O}$ and m_2, we calculate the equilibrium constant, K_2, at 4 M urea to be ~0.6 μM. This is consistent with the data shown in Figure 3, which demonstrate that dissociation occurs in the low micromolar range of protein concentration in the range of 3−5 M urea. Second, as described under Materials and Methods, the relative signals of I_2 and of I do not depend on the protein concentration, with I_2 having a larger relative signal than I. As the population of the monomeric intermediate is increased, due to dissociation of the dimeric intermediate at lower protein concentrations, the amplitude of the plateau is decreased.

DISCUSSION

Studies of protein folding have had a major impact on the understanding of protein function and the control of human disease (*29*−*32*). Caspases are the key mediators in apoptosis, a process that is absolutely necessary to maintain homeostasis in eumetazoans. While dysregulation of apop-

tosis is a common factor in a number of autoimmune diseases, neurodegenerative disorders, and cancers (*33*), learning to selectively manipulate the level of apoptosis through the activation or inhibition of caspases may well lead to therapeutic strategies for these diseases. Although poorly understood, protein−protein interactions are important for folding, dimerization, maturation, and inhibition of caspases (*34*−*38*).

We have described conditions for the equilibrium unfolding of procaspase-3 in urea-containing phosphate buffer, as monitored by both fluorescence emission and circular dichroism measurements. The folding is completely reversible, and the data demonstrated biphasic transitions, suggesting an apparent three-state unfolding process. There was a blue shift in the fluorescence emission spectrum when the protein was incubated in 4 M urea-containing buffer, suggesting that the tryptophanyl residues remain mostly buried in the equilibrium intermediate. Above 5 M urea, there was both a decrease in intensity and a red shift in the fluorescence emission spectrum, demonstrating the unfolding of the protein. When we examined unfolding at several concentrations of procaspase-3 (C163S), we observed that the midpoint for the first transition was constant, whereas the midpoint for the second transition was dependent on the protein concentration. This suggested that the second transition represents the dissociation of the dimer and that the intermediate populated between 3 and 5 M urea was a dimer. Interestingly, however, the amplitude of the plateau was also dependent on the protein concentration. While these results cannot be explained by a three-state unfolding process, they are well described by a four-state model. In this model, the native dimer isomerizes to a dimeric intermediate, and the dimeric intermediate dissociates to a monomeric intermediate, which then unfolds. The decrease in the amplitude of the plateau is a result of the dissociation of the dimeric intermediate to the monomeric intermediate. Based on this model, we have determined the conformational free energies and *m*-values for the three steps in equilibrium unfolding. The data show that the protein is very stable, with a conformational free energy of 25.8 kcal/mol, and that unfolding is a highly cooperative process.

These results show two important points. First, dimerization of procaspase-3 occurs as a result of the association of two monomeric folding intermediates. Therefore, we consider procaspase-3 dimerization to be a folding event. Second, the stability of the dimer contributes significantly to the conformational free energy of the protein (approximately 18.8 kcal/mol). These results are consistent with our previous conclusions based on the solution properties of the dimer (*44*), and we predict that the protein is also a dimer in vivo.

By using the values from the experimental data for $\Delta G_1^{H_2O}$ (8.3 ± 1.3 kcal/mol), $\Delta G_2^{H_2O}$ (10.5 ± 1.0 kcal/mol), $\Delta G_3^{H_2O}$ (7.0 ± 0.5 kcal/mol), m_1 (2.8 ± 0.5 kcal mol^{-1} M^{-1}), m_2 (0.5 ± 0.1 kcal mol^{-1} M^{-1}), and m_3 (1.2 ± 0.1 kcal mol^{-1} M^{-1}), we calculated the equilibrium distribution of the four species, N_2, I_2, I, and U, at each urea concentration. The results of these calculations are illustrated in Figure 4. In addition, the calculations were done at four protein concentrations (0.25, 0.5, 1, and 2 μM). As shown in Figure 4, between 0 and 3.5 M urea, there is a decrease in the population of native dimer and a concomitant increase in the population of the dimeric intermediate, I_2, as well as the monomeric intermediate, I. The midpoint of the transition is 2.4 M urea, consistent with the experimental results shown in Figure 3. Between 2 and 7 M urea, there is a population of I_2 as well as a population of the monomeric intermediate, I. The relative populations of the dimeric and monomeric species are dependent on the protein concentration. The population of I_2 reaches a maximum at ~3.4 M urea, whereas the population of I reaches a maximum at ~5.5 M urea. The third transition, I to U, has a midpoint at ~6.1 M urea, although there remains a significant population of I_2 and I until ~6.8 M urea. This distribution of species explains both the change in amplitude between 3 and 5 M urea as well as the protein concentration dependence between 5 and 7 M urea (Figure 3).

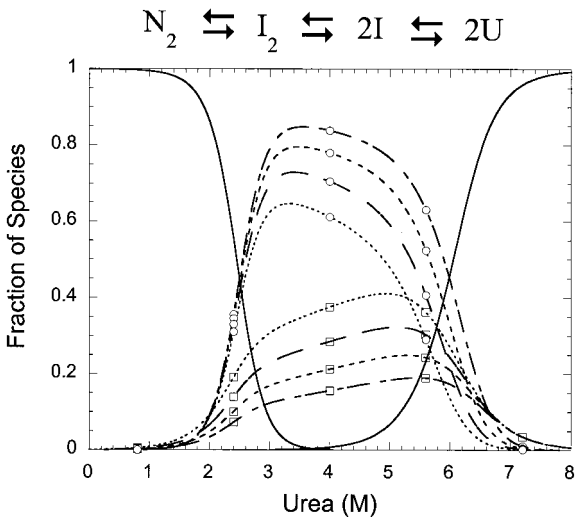

FIGURE 4: Fraction of species as a function of urea concentration. The fractions of native, dimeric intermediate, monomeric intermediate, and the unfolded protein were calculated as a function of urea concentration. The protein concentrations were 0.25 μM (•••), 0.5 μM (− −), 1 μM (- - -), and 2 μM (− - −). 'N_2' refers to the native procaspase-3(C163S), 'I_2' and 'I' are the dimeric and monomeric intermediates respectively, and 'U' refers to the unfolded species. (○) Fraction of I_2; (□) fraction of I.

According to Schellman (*39*) and Alonso and Dill (*40*), the *m*-value should be proportional to the surface area of the protein exposed to solvent upon unfolding, ΔASA. Scholtz and co-workers (*41*) have described empirical relationships that correlate ΔASA with experimental *m*-values, as shown in eq 22:

$$m = 368 + 0.11(\Delta\text{ASA}) \qquad (22)$$

Using this equation and the value determined for m_2, one can calculate the ΔASA for the transition of $I_2 \rightleftarrows 2I$ to be 1,200 Å^2. Based on the crystal structure of caspase-3 (*14*), the dimer interface between the two small subunits comprises 2000 Å^2. Given the experimental error in determining the value of m_2 (± 0.1 kcal mol^{-1} M^{-1}), our results suggest that the dimer interface may be largely intact in the dimeric intermediate, I_2. It is interesting to note that the equilibrium unfolding of procaspase-3 is unique as it represents a complex four-state model, where dissociation of the dimer and unfolding of the monomeric species do not occur simultaneously as usually observed with other oligomeric proteins (*22*, *42*).

According to Dill (*43*), proteins with homologous native conformations can fold via different structural intermediates, or pathways, to reach the homologous conformation. Although the structures of the procaspases are not known, they are likely to be similar, with the noted exceptions of the prodomains. The non-native conformations that occur during the folding of the procaspases, however, are not necessarily conserved, and thus may represent specific targets for inhibition. For example, we have found that a thermodynamically stable dimeric intermediate is present during the folding of procaspase-3. In the caspase-3 dimer, and by analogy the procaspase-3 dimer, the dominant forces linking the two monomers are hydrogen bonding interactions between the two antiparallel β-strands of the small subunits and hydrophobic interactions between Val^{266} and $Val^{266\#}$ at the 2-fold symmetry axis. In contrast, the dimer interface of procaspase-1 is very different. While the interface is also comprised of two antiparallel β-strands, it consists of four charged residues that form two salt bridges. It is not yet known whether the folding intermediate observed for procaspase-3 also exists for procaspase-1, but our data suggest that the intermediate may be very different. Thus, while the native structures are conserved, the folding pathways may differ.

REFERENCES

1. Anfinsen, C. B. (1973) *Science 181*, 223−230.
2. Baker, D. (2000) *Nature 405*, 39−42.
3. Grantcharova, V., Alm, E., Baker, D., and Horwich, A. (2001) *Curr. Opin. Struct. Biol. 11*, 70−82.
4. Jackson, S. (1998) *Folding Des. 3*, 81−91.
5. Mirny, L., and Sakhnovich, E. (1999) *J. Mol. Biol. 291*, 177−196.
6. Alnemri, E., Livingstone, D., Nicholson, D., Salvesen, G., Thornberry, N., Wong, W., and Yuan, J. (1996) *Cell 87*, 171.
7. Wolf, B. B., and Green, D. R. (1999) *J. Biol. Chem. 274*, 20049−20052.
8. Rotonda, E., Rasper, D., Ruel R, V., JP, Thornberry, N., Becker, J., Rotonda, J., Nicholson, D., Fazil, K., Gallant, M., Gareau, Y., and Labelle, M. (1996) *Nat. Struct. Biol. 7*, 619−625.
9. Walker, N. P. C., Talanian, R. V., Brady, K. D., Dang, L. C., Bump, N. J., Ferenz, C. R., Franklin, S., Ghayur, T., Hackett, M. C., and Hammill, L. D. (1994) *Cell 78*, 343−352.
10. Wilson, K. P., Black, J. A., Thomson, J. A., Kim, E. E., Griffith, J. P., Navia, M. A., Murcko, M. A., Chambers, S. P., Aldape, R. A., Raybuck, S. A., and Livingston, D. J. (1994) *Nature 370*, 270−275.
11. Watt, W., Koeplinger, K. A., Mildner, A. M., Heinrikson, R. L., Tomasselli, G., and Watenpaugh, K. D. (1999) *Structure 27*, 1135−1143.
12. Wei, Y., Fox, T., Chambers, S. P., Sintchak, J., Coll, J. T., Golec, J. M., Swenson, L., Wilson, K. P., and Charifson, P. S. (2000) *Chem. Biol. 7*, 423−432.
13. Chai, J., Shiozaki, E., Srinivasula, S., Wu, Q., Data, P., Alnemri, E., and Shi, Y. (2001) *Cell 104*, 769−780.
14. Mittl, P., Di Marco, S., Krebs, J., Bai, X., Karanewsky, D., Priestle, J., Tomaselli, K., and Grutter, M. (1997) *J. Biol. Chem. 272*, 6539−6547.
15. Stennicke, H., and Salvesen, G. (1998) *Biochim. Biophys. Acta 1387*, 17−31.
16. Ramage, P., Cheneval, D., Chvei, M., Graff, P., Hemmig, R., Heng, R., Kocher, H. P., Mackenzie, A., Memmert, K., Revesz, L., and Wishart, W. (1995) *J. Biol. Chem. 270*, 9378−9383.
17. Hoffman, K., Bucher, P., and Tschopp, J. (1992) *Trends Biochem. Sci. 22*, 155−156.
18. Chou, J., Matsuo, H., Duan, H., and Wagner, G. (1998) *Cell 94*, 171−180.
19. Yamin, T.-T., Ayala, J. M., and Miller, D. K. (1996) *J. Biol. Chem. 271*, 13273−13282.
20. Gu, Y., Wu, J., Faucheu, C., Lalanne, J. L., Diu, A., Livingston, D. J., and Su, M. S.-S. (1995) *EMBO J. 14*, 1923−1931.
21. Pace, C., Shirley, B., and Thompson, J. (1989) in *Protein Structure, A Practical Approach* (Creighton, T. E., Ed.) pp 311−330, IRL Press, New York.
22. Clark, C., Sinclair, J., and Baldwin, T. (1993) *J. Biol. Chem. 268*, 10773−10779.
23. Thompson, J., Shirley, B., Grimsley, G., and Pace, C. (1989) *J. Biol. Chem. 264*, 11614−11620.
24. Ryser, S., Vial, E., Magnenat, E., Schlegel, W., and Maundrell, K. (1999) *Curr. Genet. 36*, 21−28.
25. Fernandes-Alnemri, T., Litwack, G., and Alnemri, E. (1994) *J. Biol. Chem. 269*, 30761−30764.
26. Dorstyn, L., Kinoshita, M., and Kumar, S. (1998) *Results Probl. Cell Differ. 24*, 1−24.
27. Stennicke, H. R., Deveraux, Q. L., Humke, E. W., Reed, J. C., Dixit, V. M., and Salvesen, G. S. (1999) *J. Biol. Chem. 274*, 8359−8362.
28. Van Criekinge, W., Beyaert, R., Van de Craen, M., Vandenabeele, P., Schotte, P., De Valck, D., and Fiers, W. (1996) *J. Biol. Chem. 271*, 27245−27248.
29. Barr, P. J., and Tomei, D. L. (1994) *Bio/Technology 12*, 487−493.
30. Brown, C., Hong-Brown, L., and Welch, W. (1997) *J. Bioenerg. Biomembr. 29*, 491−502.
31. Kelly, J. (1998) *Curr. Opin. Struct. Biol. 8*, 101−106.
32. Cohen, F. E. (1999) *J. Mol. Biol. 293*, 313−320.
33. Kumar, S. (1999) *Clin. Exp. Pharmacol. Physiol. 26*, 295−303.
34. Stennicke, H., and Salvesen, G. (1997) *J. Biol. Chem. 272*, 25719−25723.
35. Thornberry, N. A., Rano, T. A., Peterson, E. P., Rasper, D. M., Timkey, T., Carcia-Calvo, M., Hotzager, V. M., Nordstrom, P. A., Roy, S., Vaillancourt, J. P., Chapman, K. T., and Nicholson, D. W. (1997) *J. Biol. Chem. 272*, 17907−17911.
36. Budihardjo, I., Oliver, H., Lutter, M., Luo, X., and Wang, X. (1999) *Annu. Rev. Cell Dev. Biol. 15*, 269−290.
37. Earnshaw, W. C., Martins, L. M., and Kaufmann, S. H. (1999) *Annu. Rev. Biochem. 68*, 383−424.
38. Garcia-Calvo, M., Peterson, E. P., Rasper, D. M., Vaillancourt, J. P., Zamboni, R., Nicholson, D. W., and Thornberry, N. A. (1999) *Cell Death Differ. 6*, 362−369.
39. Schellman, J. (1978) *Biopolymers 17*, 1305−1322.
40. Alonso, D., and Dill, K. (1991) *Biochemistry 30*, 5974−5985.
41. Myers, J., Pace, C., and Scholtz, J. (1995) *Protein Sci. 10*, 2138−2148.
42. Doyle, S., Braswell, E., and Teschke, C. (2000) *Biochemistry 39*, 11667−11676.
43. Dill, K., and Chan, H. (1997) *Nat. Struct. Biol. 4*, 10−19.
44. Pop, C., Chen, Y.-R., Smith, B., Bose, K., Bobay, B., Tripathy, A., Franzen, S., and Clark, A. C. (2001) *Biochemistry 40*, 14224−14235.

BI0110387